The Cryosphere Discuss., https://doi.org/10.5194/tc-2018-104
Manuscript under review for journal The Cryosphere
Discussion started: 9 August 2018
© Author(s) 2018. CC BY 4.0 License.

The Cryosphere Discussions
Open Access
EGU

Retreat of Thwaites Glacier, West Antarctica, over the next 100 years using various ice flow models, ice shelf melt scenarios and basal friction laws

Hongju Yu[1], Eric Rignot[1,2], Helene Seroussi[2], and Mathieu Morlighem[1]

[1]Department of Earth System Science, University of California, Irvine, California, USA
[2]Jet Propulsion Laboratory, California Institute of Technology, Pasadena, California, USA

Correspondence: Hongju Yu (hongjuy@uci.edu)

Abstract. Thwaites Glacier (TG), West Antarctica, experiences rapid, potentially irreversible grounding line retreat and mass loss in response to enhanced ice shelf melting. Several numerical models of TG have been developed recently, showing a large spread in the evolution of the glacier in the coming decades to a century. It is, however, not clear how different parameterizations of basal friction and ice shelf melt or different approximations in ice stress balance affect projections.Here, we simulate the evolution of TG using different ice shelf melt, basal friction laws and ice sheet models of varying levels of complexity to quantify the effect of these model configurations on the results. We find that the grounding line retreat and its sensitivity to ocean forcing is enhanced when a full-Stokes model is used, ice shelf melt is applied on partially floating elements, and a Budd friction is used. Initial conditions also impact the model results. Yet, all simulations suggest a rapid, sustained retreat along the same preferred pathway. The highest retreat rate occurs on the eastern side of the glacier and the lowest rate on a subglacial ridge on the western side. All the simulations indicate that TG will undergo an accelerated retreat once it retreats past the western ridge. Combining the results, we find the uncertainty is small in the first 30 years, with a cumulative contribution to sea level rise of 5 mm, similar to the current rate. After 30 years, the mass loss depends on the model configurations, with a 300% difference over the next 100 years, ranging from 14 to 42 mm.

1 Introduction

Thwaites Glacier (TG), located in the Amundsen Sea Embayment (ASE) sector of West Antarctica, is one of the largest ice dischargers in Antarctica, with a potential to raise global mean sea level by 59 cm, and one of the largest contributors to the mass loss from Antarctica (Holt et al., 2006; Mouginot et al., 2014). With a maximum speed over 4,000 m/yr and a width of nearly 120 km (Fig. 1a), the glacier discharged 126 Gt of ice into the ocean in 2014 (Mouginot et al., 2014), nearly three times as much as Jakobshavn Isbrae, the largest discharger of ice in Greenland (Howat et al., 2011). Over the past decade, the rate of mass loss of TG has increased from 28 Gt/yr in 2006 to 50 Gt/yr in 2014 (Medley et al., 2014; Mouginot et al., 2014; Rignot, 2008). The grounding line of TG has retreated by 14 km from 1992 to 2011 along its fast flowing main trunk (Rignot et al., 2014). The surface has thinned at a rate of about 4 m/yr near the grounding line and more than 1 m/yr about 100 km inland (Pritchard et al., 2009). The rate of change in mass loss increased from 2.7 Gt/yr^2 in 1978-2014 to 3.2 Gt/yr^2 in 1992-2014,

The Cryosphere Discuss., https://doi.org/10.5194/tc-2018-104
Manuscript under review for journal The Cryosphere
Discussion started: 9 August 2018
© Author(s) 2018. CC BY 4.0 License.

and 5.6 Gt/yr^2 in 2002-2014 (Mouginot et al., 2014). If these rates were to maintain over the coming decades, they would raise global sea level by, respectively, 41, 48 and 81 mm by 2100.

The rapid mass loss and grounding line retreat of TG have been attributed to an increase in ice shelf melt rate induced by warmer ocean conditions (Rignot, 2001; Joughin et al., 2014; Seroussi et al., 2017). The strengthening of westerlies around the Antarctic continent over the past decades has caused more warm, salty Circumpolar Deep Water (CDW) to intrude onto the continental shelf, flow along troughs in the sea floor, reach the sub-ice-shelf cavities and glacier grounding lines and melt them from below (Schneider and Steig, 2008; Spence et al., 2014; Dutrieux et al., 2014; Li et al., 2015; Scambos et al., 2017). An increase in ice shelf melt rate thins the ice shelves, reduces the buttressing they provide to the grounded ice, and triggers glacier speed up, yielding further thinning and retreat of the glaciers (Schoof, 2007; Goldberg et al., 2009).

For a marine-terminating glacier, bed topography also plays a crucial role in controlling the grounding line stability. According to the marine ice sheet instability (MISI) theory, in 2D, a grounding line position is stable when sitting on a prograde bed, i.e., a bed elevation that increases in the inland direction, and unstable when sitting on a retrograde bed (Weertman, 1974). In 3D, glaciers on retrograde bed are conditional stable due to the buttressing from ice shelves and lateral drag (Gudmundsson et al., 2012). The grounding line of the central trunk of TG is currently sitting on a subglacial ridge on the western part of the glacier. Upstream of the ridge, the bed is mostly retrograde until the ice divide (Fig. 1b), which indicates limited stability to changes (Hughes, 1981; Rignot et al., 2014; Joughin et al., 2014).

To assess the future of TG, we need numerical models. Based on prior studies, TG will experience continuous and rapid retreat, however, the timing and extent of the projected retreat varies significantly between models (Parizek et al., 2013; Joughin et al., 2014; Feldmann and Levermann, 2015; Seroussi et al., 2017; Rignot et al., 2014; Cornford et al., 2015). One important factor explaining the differences between models is that they employ different model configurations and ocean forcings, so it is not clear which model best captures the behavior of TG. To simulate the evolution of TG, it is important to model the grounding line migration accurately. The grounding line position is key to the stability of marine-terminating glaciers, but it is difficult to model numerically because the sharp transition from grounded ice to floating ice involves a transition in stress field (Vieli and Payne, 2005; Nowicki and Wingham, 2008; Favier et al., 2012). A full-Stokes (FS) model is required in this transition region to capture the complete ice physics (Durand et al., 2009; Morlighem et al., 2010). Most prior ice sheet models applied to TG, however, used simplified physics (Seroussi et al., 2017; Joughin et al., 2014). In that context, the treatment of ice shelf melt near the grounding line and the choice of the friction law may have a significant impact on the rate of grounding line retreat and glacier mass loss (Seroussi et al., 2014; Golledge et al., 2015; Arthern and Williams, 2017; Brondex et al., 2017).

In this study, we simulate the dynamics and evolution of TG for 100 years using the Ice Sheet System Model (ISSM) (Larour et al., 2012). To investigate the impact of different configurations, we apply three different stress balance models (FS and two approximations), two treatments of ice shelf melt near the grounding line, and two friction laws. For each of these twelve models, we employ six different ice shelf melt scenarios parameterized to match prior ocean model results and satellite observations and to encompass a realistic regime of ice shelf melt ranging from cold conditions with low access of CDW to the glacier to warm conditions with enhanced access of CDW. We compare the results from the different models and conclude on the evolution of TG over the coming century based on the model results.

The Cryosphere Discuss., https://doi.org/10.5194/tc-2018-104
Manuscript under review for journal The Cryosphere
Discussion started: 9 August 2018
© Author(s) 2018. CC BY 4.0 License.

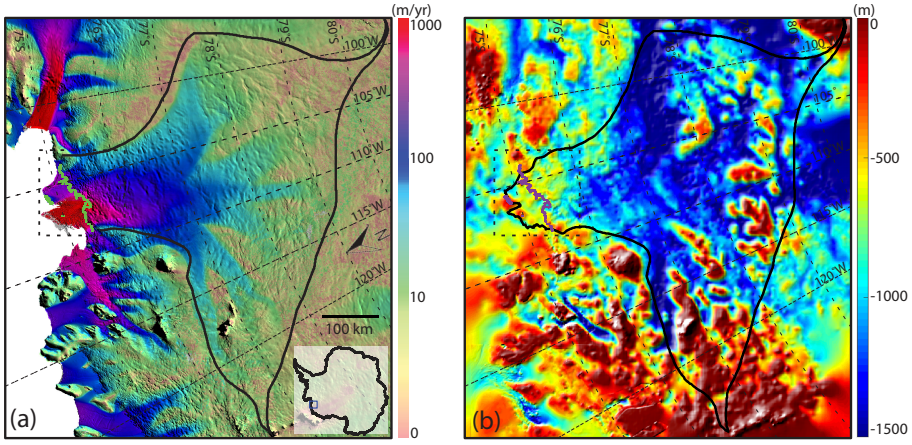

Figure 1. (a) Surface velocity of Thwaites Glacier, West Antarctica, derived from satellite radar interferometry (Rignot et al., 2011b). (b) Bed elevation of Thwaites Glacier and surrounding sea floor (Morlighem et al., 2011; Millan et al., 2017). The green line in (a) and red line in (b) are the grounding line positions in 2011 (Rignot et al., 2011a). The black contour is the drainage basin. The black dashed box in (a) is the region in Fig 4.

2 Data and methods

2.1 Data

We conduct numerical simulations of the ice flow of TG over its entire drainage basin (Fig. 1). We use BEDMAP-2 data for ice surface elevation and ice shelf draft elevation (Fretwell et al., 2013), the bed elevation from mass conservation on grounded ice (Morlighem et al., 2011, 2013) and the sea floor bathymetry from a gravity inversion beneath floating ice (Millan et al., 2017). We use the surface temperature field from the regional atmospheric climate model RACMO2.3 (Lenaerts and van den Broeke, 2012) and the geothermal heat flux from Shapiro and Ritzwoller (2004) to compute the steady state temperature field of TG (Seroussi et al., 2017). Previous studies have shown that the uncertainty in the thermal regime does not have a major impact on the evolution of glaciers within a time scale of one century (Seroussi et al., 2013). We performed some sensitivity tests (not shown here) and the model volume was within 3% of the original run at the end of the simulations. We therefore keep the thermal regime constant here. The surface mass balance is from RACMO 2.3 (Lenaerts and van den Broeke, 2012). The ice surface velocity (Fig. 1a) is from interferometric synthetic aperture radar for the year 2008 (Rignot et al., 2011b).

2.2 Ice flow models

Stress balance models. To solve the stress balance of ice flow without approximation in the stress field, we use a full-Stokes (FS) model. In addition, we use two widely-used simplified models: 1) the Higher Order (HO) model, which assumes that the horizontal gradient of the vertical velocity and the bridging effect are negligible (Blatter, 1995; Pattyn, 2003); and 2) the Shelfy-Stream Approximation (SSA) model, which is a 2D depth-averaged model, with the additional assumption that vertical

The Cryosphere Discuss., https://doi.org/10.5194/tc-2018-104
Manuscript under review for journal The Cryosphere
Discussion started: 9 August 2018
© Author(s) 2018. CC BY 4.0 License.

shear is negligible (Morland, 1987; MacAyeal, 1989). The criterion for grounding line migration differs among these models. In FS, grounding line migration is treated as a contact problem. The grounding line retreats if the normal stress at the base of the ice is smaller than the water pressure at the base. Conversely, the grounding line advances if the ice bottom tries to extend below the bed (Durand et al., 2009; Yu et al., 2017). In contrast, in HO and SSA, the grounding line position is computed solely from hydrostatic equilibrium (Seroussi et al., 2014).

Ice shelf melt treatment near grounding line. During the simulation, the position of the grounding line lies within the elements of the mesh. Numerical models implement ice shelf melt in these partially floating elements differently. Some models apply melt in proportion to the floating area fraction of each element, while some models only apply melt to fully floating elements. In our simulations, we quantify the difference between these two types of implementations by running both of them. We refer these two sets of experiments as Melt and Nomelt in the remainder of this paper.

Friction laws. We employ and compare two different friction laws. The first one is a Weertman friction law (Weertman, 1957):

$$\boldsymbol{\tau_b} = -C_w |\boldsymbol{v}_b|^{m-1} \boldsymbol{v}_b \tag{1}$$

where $\boldsymbol{\tau_b}$ is the basal drag, $\boldsymbol{v}_b$ is basal velocity and C_w is the friction coefficient. The second one is a Budd friction law (Budd et al., 1979):

$$\boldsymbol{\tau_b} = -C_b N |\boldsymbol{v}_b|^{m-1} \boldsymbol{v}_b \tag{2}$$

where N is the effective pressure at the ice base and C_b is the friction coefficient. Weertman (1957) proposed an exponent of $m = 1/3$. Here, we use a linearized version with $m = 1$ to focus on the impact of the effective pressure. However, non-linear friction laws could lead to different model behaviors. These two sets of experiments are referred to as Weertman and Budd experiments.

The ensemble of stress balance models, ice shelf melt implementations, and friction laws lead to 12 different sets of experiments.

Boundary conditions. The boundary conditions are the same for all experiments apart from the friction law. A stress free surface is applied at the ice-atmosphere interface. At the ice-ocean interface, water pressure is applied. Along the other boundaries of the model domain, Dirichlet conditions are applied to ensure that ice velocity equals the observed velocity. The calving front position is kept constant throughout our simulations.

2.3 Ice shelf melt scenarios

To simulate the response of TG to enhanced ice shelf melting, we run the model with six different ice shelf melt scenarios (Fig. 2). In all scenarios, the ice shelf melt rate is parameterized as a function of ice shelf basal elevation and is set to 0 above

The Cryosphere Discuss., https://doi.org/10.5194/tc-2018-104
Manuscript under review for journal The Cryosphere
Discussion started: 9 August 2018
© Author(s) 2018. CC BY 4.0 License.

150 m depth. In the first scenario, the ice shelf melt rate linearly increases to a maximum of 80 m/yr at 1000 m depth. Below 1000 m depth, the ice shelf melt rate is kept constant at 80 m/yr. This scenario originates from simulations using the coupled ISSM/MITgcm ice-ocean model for year 1992 (Seroussi et al., 2017). Year 1992 was a cold year with a low ice shelf melt rate in ASE compared to the average over the past 30 years (Schodlok et al., 2012), which makes this scenario representative of relatively cold ocean conditions. With this parameterization, the mass loss from ice shelf melt for TG is 73.7 Gt/yr at the beginning of the simulation. This value is close to the estimated ice shelf melt of 69 Gt/yr from Depoorter et al. (2013) and 24% less than the 97.5 Gt/yr for the years 2003-2008 in Rignot et al. (2013) .

In the other five scenarios, we change the maximum ice shelf melt rate and the depth where the maximum melt occurs. To constrain the range of ice shelf melt rates, we calculate the ice shelf melt rate with mass conservation as in (Rignot et al., 2013) using the 2008 velocity, ice shelf thickness from BEDMAP-2, and the bathymetry of ASE to find a maximum ice shelf melt rate at 125 m/yr, or 50% larger than the first scenario. In 2007, which was a warm year, the nearby Pine Island Glacier experienced ∼50 % more melt compared to 1992 (Schodlok et al., 2012). Therefore, in the second scenario, we increase the maximum ice shelf melt rate by 50 % to 120 m/yr to represent warm ocean conditions. Jacobs et al. (2012) showed that in 2007, the thermal forcing, which is the difference between the *in-situ* ocean temperature and the *in-situ* freezing point of seawater, exceeded +4°C at the ice front of TG, which implied almost undiluted CDW. This indicates that the potential of further increase in ice shelf melt rate is limited. Therefore, in the third scenario, we choose to increase the maximum ice shelf melt rate by another 40 m/yr to 160 m/yr to represent extreme warmth. We also vary the depth at which the ice shelf melt rate reaches its maximum. Ocean observations show that the bottom of the thermocline has been relatively constant at 700 m depth in the past two decades in ASE (Dutrieux et al., 2014). Accordingly, we run three additional ice shelf melt scenarios with the maximum ice shelf melt rate (80 m/yr, 120 m/yr, 160 m/yr) occurs below 700 m instead of 1000 m (Fig. 2).

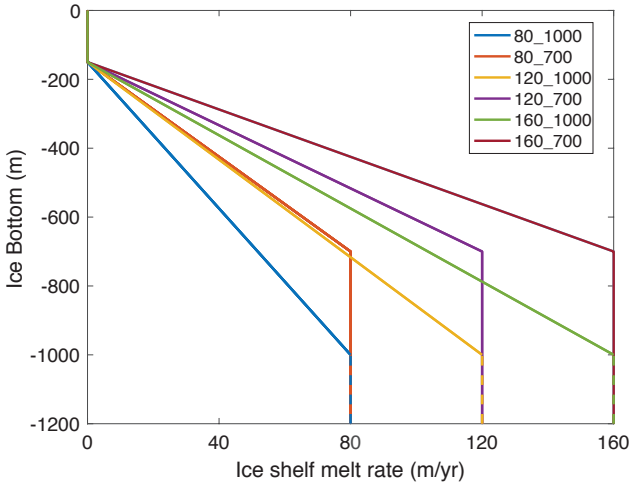

Figure 2. Ice shelf melt rate parameterization of the six ocean forcing scenarios.

The Cryosphere Discuss., https://doi.org/10.5194/tc-2018-104
Manuscript under review for journal The Cryosphere
Discussion started: 9 August 2018
© Author(s) 2018. CC BY 4.0 License.

Overall, we run a total of 72 simulations (6 ice shelf melt scenarios by 12 models). We name our simulations from the combination of their ice shelf melt scenario, stress balance equation, ice shelf melt treatment and friction law. For instance, Exp. 80_1000_FS_Nomelt_Budd represents the experiment conducted with a maximum of 80 m/yr ice shelf melt rate below 1000 m depth, FS stress balance model, ice shelf melt only applied to fully floating elements, and a Budd friction law.

2.4 Initial model setup

The mesh is constructed using an anisotropic metric based on ice surface velocity and distance to the grounding line, and comprises the entire drainage basin of TG. The horizontal mesh spacing is 300 m in the grounding line region, progressively increasing to 10 km in the interior of the ice sheet. Vertically, the domain is divided into 8 vertical layers that are denser at the bottom. In total, our mesh includes 561,799 triangular prismatic elements.

In order to relax the model while maintaining a good fit with surface observations, we adopt the following procedure. We first conduct an inversion of the basal friction coefficient over the grounded ice and of the ice viscosity parameter over the floating ice to best match modeled surface velocity with the observed surface velocity (Morlighem et al., 2010). After the inversion, we find a rapid change in ice velocity of a few 100 m/yr at the grounding line in transient simulations due to inconsistencies between datasets (Seroussi et al., 2011). To avoid this problem, we run the model for 0.5 yr to relax the model and perform a second inversion. We repeat this procedure 4 times until we reach a stable solution. After these iterative steps, the modeled velocity is consistent with observations at the beginning of transient simulations, within 50 m/yr (Fig. 3). Note that the inversions for ice viscosity parameter and basal friction are conducted independently for the three ice flow models so that each model has its own, self-consistent initial set up. The inversions are conducted with the Weertman friction law. For the Budd friction law, the friction coefficient is computed directly through $C_b = C_w/N$ to ensure same initial basal conditions for the two sets of experiments.

FS is more sensitive to mesh resolution than HO and SSA and requires a higher mesh resolution in the interior than other models in order to converge. To avoid the computational cost of a high resolution FS modeling over the entire basin, we use a tiling method to apply FS within 150 km of the grounding line and HO in the interior (Seroussi et al., 2012). In this manner, we insure that the FS model is computationally efficient, the results are reliable, and the regions where the grounding line retreats are modeled using FS.

3 Results

Inversion. The inversion results are shown in Fig. 3. The pattern of basal friction is the same for all models, with high friction near the ice divide and low friction in the deep basin. SSA needs a smaller friction coefficient than HO and FS to match observed velocity because of the neglected vertical shear. The inferred ice viscosity parameter over floating ice is also similar for the three models with stiff ice near the grounding line and soft ice at the junction between the eastern ice shelf and the main trunk. After the inversion, the mismatch between modeled and observed surface velocity is small, i.e. within 200 m/yr in the fast moving region and within 30 m/yr for HO and SSA in the interior. For FS, the difference is large in the interior, about 100

The Cryosphere Discuss., https://doi.org/10.5194/tc-2018-104
Manuscript under review for journal The Cryosphere
Discussion started: 9 August 2018
© Author(s) 2018. CC BY 4.0 License.

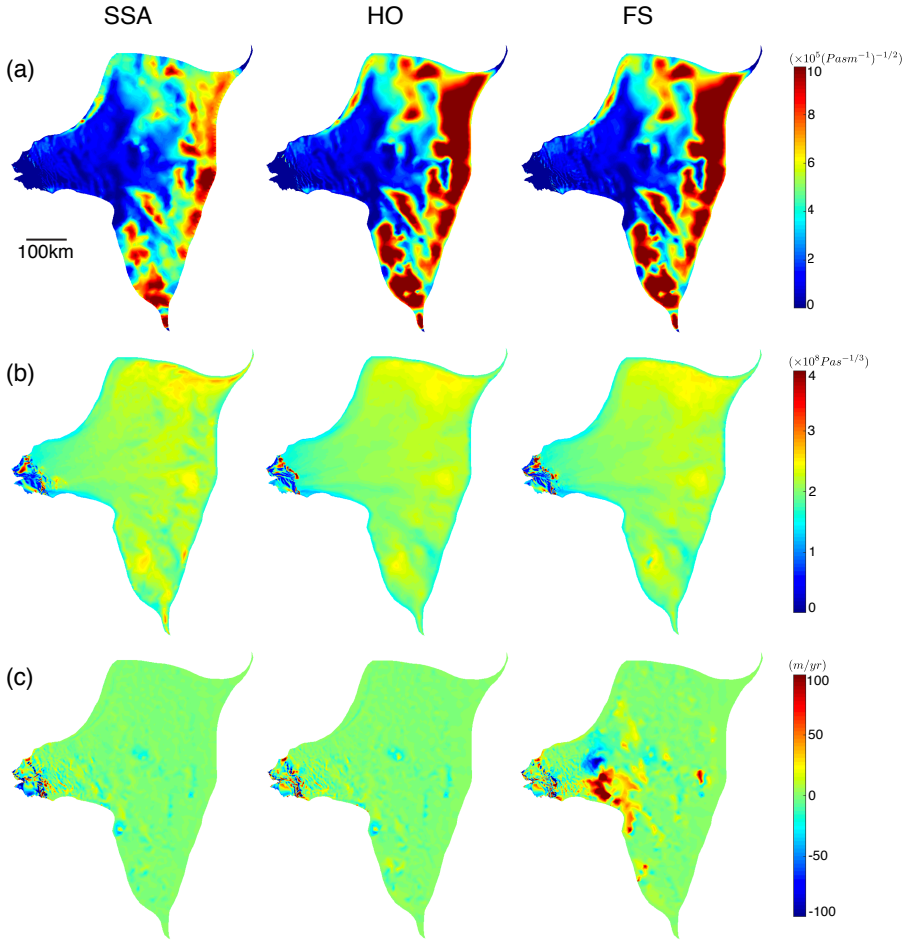

Figure 3. Inversion results. a) Basal friction coefficient inferred for SSA (left column), HO (middle column) and FS (right column) models. b) Depth-average ice viscosity parameter for the three models, combined with thermal model output over grounded ice and inversion results over floating ice. c) Difference between modeled and observed surface velocity for the three models.

m/yr due to the tiling method, but this difference has limited impact on our results since it takes place far from the grounding line region (>100 km) and the changes in that region are relatively small.

Grounding line retreat and mass loss. In transient simulations, the results display a consistent, general pattern of retreat, with different magnitude of mass loss and rates of grounding line retreat. Overall, the grounding line retreats faster on the eastern side of the glacier and tends to remain stable on the western side. A sustained mass loss is obtained for all simulations.

The evolution of the grounding line positions for all 12 models with the lowest (80_1000) and highest ice shelf melt (160_700) scenarios are shown in Fig. 4. The grounding line retreat shows distinct features on the eastern and western sides due to bed topography. On the eastern side, the grounding line retreats continuously in all experiments for 30-65 km. The main

© Author(s) 2018. CC BY 4.0 License.

difference among the simulations is whether and when the grounding line retreats over the subglacial ridge 35 km upstream of its present location. On the western side, the grounding line is stable with only small retreat in all cases except for the Melt experiments in high ice shelf melt scenarios. However, once the grounding line starts to retreat in the west, it retreats rapidly at more than 1 km/yr. The changes in grounded area are consistent with the grounding line migration (Fig. 5), i.e., limited change when the grounding line sits on a subglacial ridge and faster change when the grounding line retreats along retrograde or flat bed.

The mass loss is significant and rapid in all simulations (Fig. 5). The loss in volume above flotation (VAF) is closer to linear than grounded area loss due to the relatively constant thinning rate in the interior. Combining all simulations, the VAF loss is equivalent to a 15–42 mm global mean sea level (GMSL) rise in 100 years.

Difference among simulations. The response of TG to ocean melting differs when using different stress balance models, ice shelf melt implementations and friction laws. Among the three stress balance models, FS shows more grounding line retreat than HO and SSA, except in the Melt_Weertman experiments, where HO retreats the most. In the Nomelt and Melt_Budd experiments, FS produces 5-40% more grounded area loss than HO and SSA. In the Melt_Weertman experiments, FS has 10% less retreat than HO and 15% more than SSA. In the VAF loss perspective, the three models are closer to each other. SSA shows more VAF loss in the Budd experiments, while FS shows more VAF loss in the Weertman experiments. The overall differences are within 20%.

The grounding line retreat rate is significantly reduced in the Nomelt experiments compared to the Melt experiments. The total grounded area loss is reduced by 35-65% and the VAF loss is reduced by 15-40%. The choice of friction law also has a significant impact on the results. The Budd friction law produces more grounding line retreat (10-50%) and more VAF loss (15-90%) than the Weertman friction law. The Budd experiments also display a higher sensitivity to ocean forcing than the Weertman experiments.

Different ice shelf melt scenarios have significant impact on the behavior of TG. A higher ice shelf melt rate always leads to more retreat. However, the sensitivity to changes in ice shelf melt rate varies among the models. The Melt experiments with FS or HO and Budd friction law are more sensitive to ocean forcing than the Nomelt experiments with SSA and Weertman friction law.

4 Discussion

Impact of the stress balance models. In our simulations, the stress balance models produce different results for several reasons. First, the model physics are different. With the inclusion of vertical shear and bridging effects in the stress field, the ice viscosity in FS is lowered, which leads to a larger acceleration as the grounding line retreats. In the MISMIP3D experiments, for example, using the same initial setting, the modeled ice velocity of FS is faster than HO by 0-5%, and HO is faster than SSA by another 0-5% (Pattyn et al., 2013). Second, the grounding line positions are computed differently. For HO and SSA, it is computed through hydrostatic equilibrium, which compares the bottom water pressure with the overburden ice pressure.

The Cryosphere Discuss., https://doi.org/10.5194/tc-2018-104
Manuscript under review for journal The Cryosphere
Discussion started: 9 August 2018
© Author(s) 2018. CC BY 4.0 License.

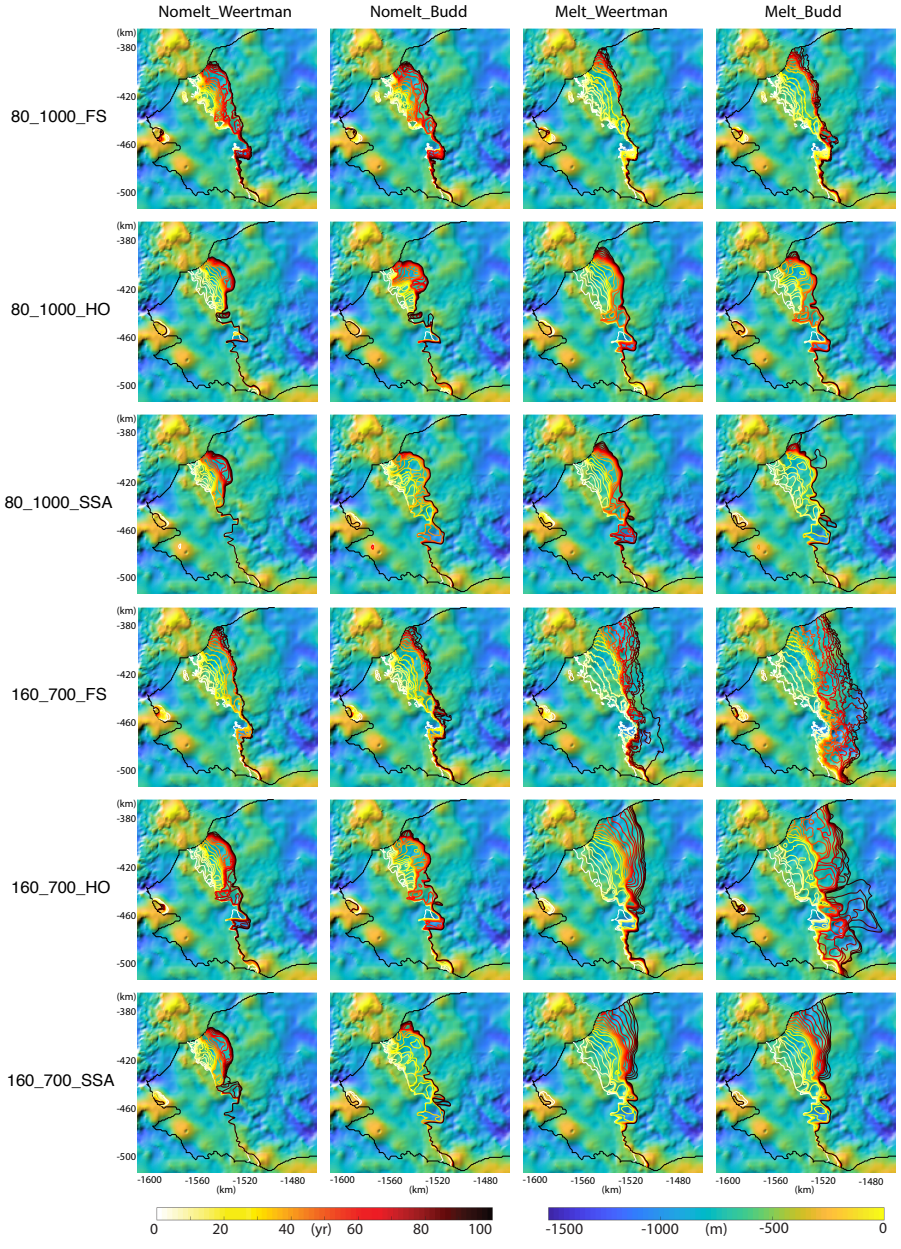

Figure 4. Grounding line evolution of all 12 models with the two end members ice shelf melt scenarios, overlaid on the bed elevation map of Thwaites Glacier, West Antarctica. Each panel represents one simulation. Within each panel, the grounding line positions are plotted every 5 years.

For FS, the bottom water pressure is compared with the normal stress at the base, which deviates from the overburden ice pressure by a few percent. In the grounding line region, and in particular, in the bending zone of the glacier, ice is pushed

The Cryosphere Discuss., https://doi.org/10.5194/tc-2018-104
Manuscript under review for journal The Cryosphere
Discussion started: 9 August 2018
© Author(s) 2018. CC BY 4.0 License.

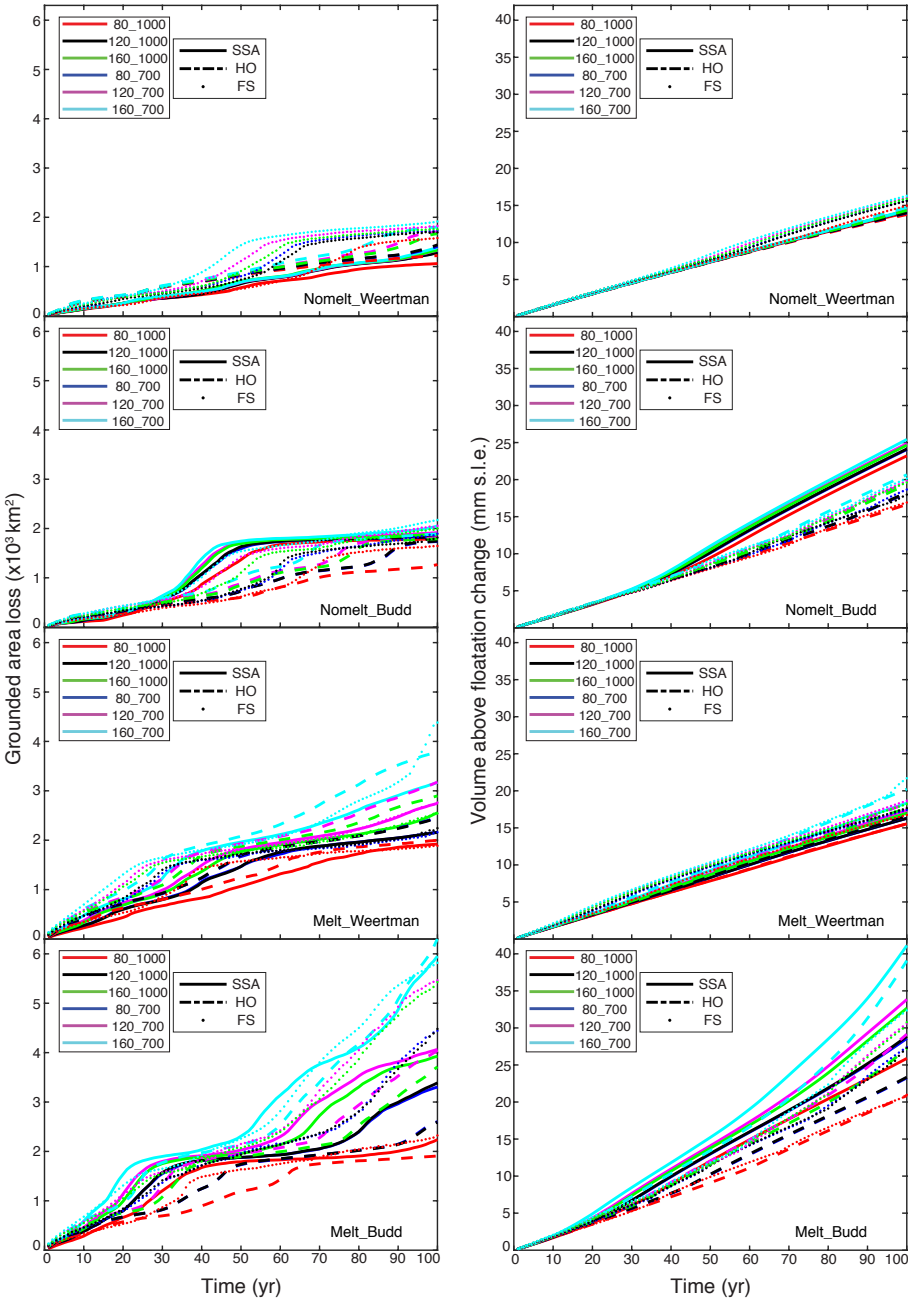

Figure 5. Grounded area loss (left column) and volume above flotation (VAF) loss (right column) of Thwaites Glacier, West Antarctica for the 72 experiments over the 100 year simulation.

© Author(s) 2018. CC BY 4.0 License.

below hydrostatic equilibrium because of the bending moment of ice as it tries to reach hydrostatic equilibrium in the ocean water (Rignot, 2001; Yu et al., 2017). As a result of this non-hydrostatic condition, the vertical velocity is high downstream of the grounding line, which produces high vertical shear that decreases the normal stress at the base. Moreover, the horizontal stretching of ice is large in the grounding line region, which reduces the normal stress at the ice base (van der Veen and Whillans, 1989; Pattyn et al., 2013).

Numerical issues also contribute to the differences between the models. We conduct inversions for each model separately to make sure that they best fit the observations. Hence, the initial conditions are slightly different for each model, which sets them up on different trajectories. In transient simulations, small differences in initial conditions may accumulate with time and lead to further significant differences in the model outcomes. Here, SSA has a higher rate of VAF loss than grounded area loss with respected to HO and FS. This is due to the higher thinning rate in the interior simulated by SSA. This sensitivity to initial conditions indicates that we need better constraints for the inversion process. For instance, we should infer the basal friction coefficient and ice viscosity parameter using a series of observed velocities, as in Goldberg et al. (2015), rather than a single velocity map.

In summary, the FS model has more complex physics compared to HO and SSA and leads to faster grounding line retreat, especially over subglacial ridges. The difference between FS and simplified models depends on the bed topography. The limitation of FS is computational. FS is 10 times slower than HO and 100 times slower than SSA. In our results, however, the impact of different stress balance models is smaller than the impact of ice shelf melt treatment and friction law. Meanwhile, initial conditions are also critical to consider when comparing model results.

Impact of the ice shelf melt treatment near grounding line. Our results also show that if we apply ice shelf melt in the partially floating elements, the results change significantly, which is consistent with previous studies (Golledge et al., 2015; Arthern and Williams, 2017). Theoretically, these two methods should have the same results if the mesh resolution is small enough. However, this is not achieved with our 300 m resolution and may therefore be difficult to achieve numerically. For the partially floating elements, it is expected that some ice shelf melt would occur in the floating portion, so not applying any ice shelf melt might underestimate the mass loss. In the newly ungrounded cavity, the ice shelf melt rate may not be as high as the previously floating area due to its limited access to warm water. The removal of ice at the base in partially floating elements may also lead to unrealistic thinning upstream of the grounding line due to the implementation of the mass transport equation. Therefore, the model may overestimate mass loss if ice shelf melt is applied in the partially floating elements. We also conducted the same simulation with coarser and finer mesh resolutions with SSA and the Nomelt experiments are showing less sensitivity to mesh resolutions than the Melt experiments.

Impact of the friction laws. The introduction of an effective pressure term in the Budd friction law produces more retreat and mass loss compared to the Weertman experiments. With the Budd friction law, the basal drag is reduced when the ice is thinning, which in turn accelerates further retreat and thinning, forming a positive feedback. In our results, the difference between Weertman and Budd experiments is larger in VAF loss than grounded area loss due to the changes in the interior. Once

© Author(s) 2018. CC BY 4.0 License.

the friction is reduced with the Budd friction law, ice thinning increases and propagates inland to produce more VAF loss than with the Weertman experiments. This result indicates that the difference in grounding line retreat between these two sets of experiments diverges with time as the upstream thinning signal evolves.

The underlying assumption for the Budd friction law is the existence of a subglacial drainage system. Previous studies have revealed that such systems exist in West Antarctica and are connected to the ocean (Gray et al., 2005; Fricker et al., 2007; Le Brocq et al., 2013). Therefore, it might be more reasonable to use a Budd friction law in the grounding line region of TG. However, in the interior ice sheet, such drainage system may not be present and the use of a Budd friction law could overestimate the total mass loss. Recently, Tsai et al. (2015) proposed a friction law that incorporates both a Weertman friction law and a Coulomb friction law, which might work for both the grounding line and the interior regions. This method requires two sets of basal friction coefficients, which is difficult to infer in a real glacier and remains beyond the scope of this study.

Impact of bed topography and ocean forcing. Despite the differences between these models, the overall results are similar as the glacier retreats along the same preferred paths. The major difference between the models is on the time it takes for each model to overcome ridges in bed topography along the pathway of the retreat. In all simulations, TG experiences grounding line retreat and mass loss over the entire period, which is consistent with previous studies (Joughin et al., 2014; Feldmann and Levermann, 2015; Seroussi et al., 2017). The retreat rate is highly dependent on bed topography. On the eastern side, there are three subglacial ridges that provide temporary stability to the glacier. The current grounding line position is on the retrograde side of the first ridge on the east. The second ridge is 35 km upstream. In the Nomelt experiments, the grounding line positions are still sitting on this ridge after 100 years. In the Melt experiments, all simulations except the 80_1000 ones have their grounding line retreat over this ridge, with the timing varying from 55 to 90 years. The third ridge is another 25 km upstream. None of our simulations show grounding line retreats over this ridge within one century. The slope of the third ridge is similar to the second ridge. We therefore expect this ridge to have a similar stabilizing effect as the second ridge.

The subglacial ridge that has the strongest stabilizing effect is the western subglacial ridge where the grounding line is currently sitting on. In the Nomelt experiments, the grounding lines are stable in the west. In the Melt_Weertman experiments, only the FS model with the highest ice shelf melt rate has its grounding line retreat over the ridge at year 95. In the Melt_Budd experiments, the grounding line retreats over this ridge for the three high ice shelf melt scenarios (160_700, 160_1000, 120_700). Further upstream, the bed slope of TG is retrograde until the ice divide. Once the grounding line retreats over the western ridge, it is not clear how the retreat of the grounding line could be stopped.

The impact of ocean forcing is most significant in the Melt_Budd experiments and is relatively small in the Nomelt experiments. The difference is due to the grounding line retreat rate in these experiments. In the scenario where the grounding line is constantly retreating, a higher ice shelf melt rate will remove ice in the newly ungrounded area more rapidly and reduces the buttressing force on the inland ice faster, which leads to further retreat. If the grounding line position is relatively stable, however, a higher ice shelf melt rate will only act over floating ice. The removal of ice is limited in this region as the ice bottom evolves to a steady shape and the reduction of buttressing becomes limited.

© Author(s) 2018. CC BY 4.0 License.

In our simulations, the effect of changing the depth of maximum melt from 1000 m to 700 m is similar to increasing the maximum ice shelf melt rate by 50% (80_700 v.s. 120_1000 and 120_700 v.s. 160_1000). This is because the bed elevation between the current grounding line and the upstream subglacial ridges is between 800 and 500 m depth, which makes the melt rate at this depth particularly important. If warm ocean water intrudes at 700 m depth, as observed on Pine Island Glacier, or above, the retreat of TG will be more rapid, even without increasing the maximum ice shelf melt rate. Indeed, the bathymetry in Millan et al. (2017) suggests that the main points of entry of CDW into the sub-ice-shelf cavities of TG have a maximum depth of 700 m.

Contribution to global sea level rise. The contribution to global sea level rise revealed by our simulations spread a large range from 14 to 42 mm in the next 100 years. However, in the first 30 years, all models suggests a global sea level rise of 5 mm, or 0.18 mm/yr. This rate is consistent with the satellite observations of 0.14 mm/yr in 2014, which kept increasing in the past decades. Previous modeling studies also have similar estimations, ranging from 0.15 mm/yr to 0.25 mm/yr (Joughin et al., 2010; Cornford et al., 2015; Seroussi et al., 2017). After 30 years, the retreat of TG would continue, whether the retreat rate will accelerate is highly dependent on the numerical model used and a longer time record of observations are needed to know which model best reproduce the observational period.

Limitations of the model study. One limitation of this model study is the ice shelf melt rate parameterization. It would be preferable to apply ice shelf melt rate calculated using a coupled ice-ocean model, i.e. with a time-dependent cavity (Seroussi et al., 2017; Cornford et al., 2015). Coupled models indicate that warm ocean water has more limited access to newly formed cavities as ice retreats (De Rydt and Gudmundsson, 2016; Seroussi et al., 2017). This lower efficiency of ice shelf melt will lower the contribution of TG to sea level rise in the 21st century.

Similarly, ice front migration is not included in our simulations. We assume that the ice front position of TG remains fixed so that all ice passing the present day ice front immediately calves. Densely distributed crevasses along the ice shelf of TG, however, make the ice shelf conducive to rapid calving (Yu et al., 2017). Once the ice shelf is removed, the grounding line will retreat into deeper regions, and the probability of calving increases according to the marine ice-cliff instability theory (Pollard et al., 2015; Wise et al., 2017). Crevassing and calving will therefore reduce ice shelf buttressing drastically and accelerate ice flow further, which means that our simulations underestimate the potential mass loss of TG (MacGregor et al., 2012). On Pine Island Glacier, calving has increased in frequency and its ice front is now 35 km farther inland on the eastern side than in the 1940's (MacGregor et al., 2012; Jeong et al., 2016). On TG, the floating ice tongue in the center trunk has retreated by 26 km from 1973 to 2009 (MacGregor et al., 2012). The eastern ice shelf has been thinning and retreating, which means that the ice shelf may disintegrate in the coming decades.

The Cryosphere Discuss., https://doi.org/10.5194/tc-2018-104
Manuscript under review for journal The Cryosphere
Discussion started: 9 August 2018
© Author(s) 2018. CC BY 4.0 License.

5 Conclusions

We simulate the response of Thwaites Glacier, West Antarctica to varying model configurations and ice shelf melt scenarios. We find that the stress balance approximations, the treatment of ice shelf melt near the grounding line, the friction law, and the ice shelf melt rate parameterization all affect the retreat of TG significantly. Different model configurations affect the results mainly through the timing for the grounding line to retreat past subglacial ridges; different ice shelf melt rates mainly affect the retreat rate when the grounding line is retreating along retrograde portions of the bed. Despite the differences, however, all models follow similar trajectories and concur to indicate that TG will continue to retreat at a rapid rate over the next century, under both cold and warm ocean water scenarios. The retreat is controlled by the bed topography. Subglacial ridges on the eastern side will only moderately delay the retreat, whereas the western ridge provides the most stability for the glacier, for at least the next several decades. Once the grounding line retreats past the western subglacial ridge, our simulations suggest that there will be no further stabilization of the glacier and the retreat will become unstoppable over the next 100 years. Our simulations project a 5 mm global mean sea level contributions from TG in the next 30 years, and 14-42 mm in the next 100 years.

Code and data availability. The ice flow model ISSM can be found and downloaded at https://issm.jpl.nasa.gov/ (Larour et al., 2012). The input data can be found and downloaded at http://faculty.sites.uci.edu/erignot/data/

Competing interests. The authors declare that there is no conflict of interest.

Acknowledgements. This work was carried out at the University of California Irvine and at the Jet Propulsion Laboratory, California Institute of Technology under a contract with the Cryosphere Science Program of the National Aeronautics and Space Administration.

© Author(s) 2018. CC BY 4.0 License.

References

Arthern, R. J. and Williams, C. R.: The sensitivity of West Antarctica to the submarine melting feedback, Geophys. Res. Lett., 44, 2352–2359, https://doi.org/10.1002/2017GL072514, 2017.

Blatter, H.: Velocity And Stress-Fields In Grounded Glaciers: A Simple Algorithm For Including Deviatoric Stress Gradients, J. Glaciol., 41, 333–344, 1995.

Brondex, J., Gagliardini, O., Gillet-Chaulet, F., and Durand, G.: Sensitivity of grounding line dynamics to the choice of the friction law, J. Glaciol., 63, 854–866, https://doi.org/10.1017/jog.2017.51, 2017.

Budd, W. F., Keage, P. L., and Blundy, N. A.: Empirical studies of ice sliding, J. Glaciol., 23, 157–170, 1979.

Cornford, S. L., Martin, D. F., Payne, A. J., Ng, E. G., Le Brocq, A. M., Gladstone, R. M., Edwards, T. L., Shannon, S. R., Agosta, C., Van Den Broeke, M. R., Hellmer, H. H., Krinner, G., Ligtenberg, S. R. M., Timmermann, R., and Vaughan, D. G.: Century-scale simulations of the response of the West Antarctic Ice Sheet to a warming climate, The Cryosphere, 9, 1579–1600, https://doi.org/10.5194/tc-9-1579-2015, 2015.

De Rydt, J. and Gudmundsson, G. H.: Coupled ice shelf-ocean modeling and complex grounding line retreat from a seabed ridge, J. Geophys. Res. Earth Surf., 121, 865–880, https://doi.org/10.1002/2015JF003791, https://agupubs.onlinelibrary.wiley.com/doi/abs/10.1002/2015JF003791, 2016.

Depoorter, M. a., Bamber, J. L., Griggs, J. a., Lenaerts, J. T. M., Ligtenberg, S. R. M., van den Broeke, M. R., and Moholdt, G.: Calving fluxes and basal melt rates of Antarctic ice shelves., Nature, 502, 89–92, https://doi.org/10.1038/nature12567, 2013.

Durand, G., Gagliardini, O., de Fleurian, B., Zwinger, T., and Le Meur, E.: Marine ice sheet dynamics: Hysteresis and neutral equilibrium, J. Geophys. Res., 114, 1–10, https://doi.org/10.1029/2008JF001170, 2009.

Dutrieux, P., De Rydt, J., Jenkins, A., Holland, P. R., Ha, H. K., Lee, S. H., Steig, E. J., Ding, Q., Abrahamsen, E. P., and Schröder, M.: Strong sensitivity of Pine Island ice-shelf melting to climatic variability., Science, 343, 174–8, https://doi.org/10.1126/science.1244341, 2014.

Favier, L., Gagliardini, O., Durand, G., and Zwinger, T.: A three-dimensional full Stokes model of the grounding line dynamics: effect of a pinning point beneath the ice shelf, The Cryosphere, 6, 101–112, https://doi.org/10.5194/tc-6-101-2012, 2012.

Feldmann, J. and Levermann, A.: Collapse of the West Antarctic Ice Sheet after local destabilization of the Amundsen Basin, Proc. Natl. Acad. Sci. USA, 112, 14 191–14 196, https://doi.org/10.1073/pnas.1512482112, 2015.

Fretwell, P., Pritchard, H. D., Vaughan, D. G., Bamber, J. L., Barrand, N. E., Bell, R., Bianchi, C., Bingham, R. G., Blankenship, D. D., Casassa, G., Catania, G., Callens, D., Conway, H., Cook, a. J., Corr, H. F. J., Damaske, D., Damm, V., Ferraccioli, F., Forsberg, R., Fujita, S., Gim, Y., Gogineni, P., Griggs, J. a., Hindmarsh, R. C. a., Holmlund, P., Holt, J. W., Jacobel, R. W., Jenkins, A., Jokat, W., Jordan, T., King, E. C., Kohler, J., Krabill, W., Riger-Kusk, M., Langley, K. a., Leitchenkov, G., Leuschen, C., Luyendyk, B. P., Matsuoka, K., Mouginot, J., Nitsche, F. O., Nogi, Y., Nost, O. a., Popov, S. V., Rignot, E., Rippin, D. M., Rivera, A., Roberts, J., Ross, N., Siegert, M. J., Smith, a. M., Steinhage, D., Studinger, M., Sun, B., Tinto, B. K., Welch, B. C., Wilson, D., Young, D. a., Xiangbin, C., and Zirizzotti, A.: Bedmap2: improved ice bed, surface and thickness datasets for Antarctica, The Cryosphere, 7, 375–393, 2013.

Fricker, H. A., Scambos, T., Bindschadler, R., and Padman, L.: An active subglacial water system in West Antarctica mapped from space, Science, 315, 1544–1548, https://doi.org/10.1126/science.1136897, 2007.

Goldberg, D., Holland, D. M., and Schoof, C.: Grounding line movement and ice shelf buttressing in marine ice sheets, J. Geophys. Res., 114, 1–23, https://doi.org/10.1029/2008JF001227, 2009.

© Author(s) 2018. CC BY 4.0 License.

Goldberg, D. N., Heimbach, P., Joughin, I., and Smith, B.: Committed retreat of Smith, Pope, and Kohler Glaciers over the next 30 years inferred by transient model calibration, The Cryosphere, 9, 2429–2446, https://doi.org/10.5194/tc-9-2429-2015, 2015.

Golledge, N. R., Kowalewski, D. E., Naish, T. R., Levy, R. H., Fogwill, C. J., and Gasson, E. G.: The multi-millennial Antarctic commitment to future sea-level rise, Nature, 526, 421–425, https://doi.org/10.1038/nature15706, 2015.

Gray, L., Joughin, I., Tulaczyk, S., Spikes, V. B., Bindschadler, R., and Jezek, K.: Evidence for subglacial water transport in the West Antarctic Ice Sheet through three-dimensional satellite radar interferometry, Geophys. Res. Lett., 32, 1–4, https://doi.org/10.1029/2004GL021387, 2005.

Gudmundsson, G. H., Krug, J., Durand, G., Favier, L., and Gagliardini, O.: The stability of grounding lines on retrograde slopes, The Cryosphere, 6, 1497–1505, https://doi.org/10.5194/tc-6-1497-2012, 2012.

Holt, J. W., Blankenship, D. D., Morse, D. L., Young, D. A., Peters, M. E., Kempf, S. D., Richter, T. G., Vaughan, D. G., and Corr, H. F. J.: New boundary conditions for the West Antarctic Ice Sheet: Subglacial topography of the Thwaites and Smith glacier catchments, Geophys. Res. Lett., 33, 1–4, https://doi.org/10.1029/2005GL025561, 2006.

Howat, I. M., Ahn, Y., Joughin, I., van den Broeke, M. R., Lenaerts, J. T. M., and Smith, B.: Mass balance of Greenland's three largest outlet glaciers, 2000-2010, Geophys. Res. Lett., 38, 1–5, https://doi.org/10.1029/2011GL047565, 2011.

Hughes, T.: The weak underbelly of the West Antarctic ice-Sheet, J. Glaciol., 27, 518–525, 1981.

Jacobs, S., Jenkins, A., Hellmer, H., Giulivi, C., Nitsche, F., Huber, B., and Guerrero, R.: The Amundsen Sea and the Antarctic Ice Sheet, Oceanography, 25, 154–163, https://doi.org/10.5670/oceanog.2012.90, 2012.

Jeong, S., Howat, I. M., and Bassis, J. N.: Accelerated ice shelf rifting and retreat at Pine Island Glacier, West Antarctica, Geophys. Res. Lett., 43, 11,720–11,725, https://doi.org/10.1002/2016GL071360, 2016.

Joughin, I., Smith, B. E., Howat, I. M., Scambos, T., and Moon, T.: Greenland flow variability from ice-sheet-wide velocity mapping, J. Glaciol., 56, 416–430, 2010.

Joughin, I., Smith, B. E., and Medley, B.: Marine ice sheet collapse potentially under way for the Thwaites Glacier Basin, West Antarctica., Science, 344, 735–8, https://doi.org/10.1126/science.1249055, 2014.

Larour, E., Seroussi, H., Morlighem, M., and Rignot, E.: Continental scale, high order, high spatial resolution, ice sheet modeling using the Ice Sheet System Model (ISSM), J. Geophys. Res., 117, 1–20, https://doi.org/10.1029/2011JF002140, 2012.

Le Brocq, A. M., Ross, N., Griggs, J. A., Bingham, R. G., Corr, H. F. J., Ferraccioli, F., Jenkins, A., Jordan, T. A., Payne, A. J., Rippin, D. M., and Siegert, M. J.: Evidence from ice shelves for channelized meltwater flow beneath the Antarctic Ice Sheet, Nature Geoscience, 6, 945–948, https://doi.org/10.1038/ngeo1977, 2013.

Lenaerts, J. T. M. and van den Broeke, M. R.: Modeling drifting snow in Antarctica with a regional climate model: 2. Results, J. Geophys. Res., 117, D05 109, https://doi.org/10.1029/2010JD015419, 2012.

Li, X., Holland, D. M., Gerber, E. P., and Yoo, C.: Rossby waves mediate impacts of tropical oceans on west Antarctic atmospheric circulation in austral winter, Journal of Climate, 28, 8151–8164, https://doi.org/10.1175/JCLI-D-15-0113.1, 2015.

MacAyeal, D. R.: Large-scale ice flow over a viscous basal sediment: Theory and application to Ice Stream B, Antarctica, J. Geophys. Res., 94, 4071–4087, 1989.

MacGregor, J. A., Catania, G. A., Markowski, M. S., and Andrews, A. G.: Widespread rifting and retreat of ice-shelf margins in the eastern Amundsen Sea Embayment between 1972 and 2011, J. Glaciol., 58, 458–466, 2012.

Medley, B., Joughin, I., Smith, B. E., Das, S. B., Steig, E. J., Conway, H., Gogineni, S., Lewis, C., Criscitiello, A. S., McConnell, J. R., van den Broeke, M. R., Lenaerts, J. T. M., Bromwich, D. H., Nicolas, J. P., and Leuschen, C.: Constraining the recent mass balance of

© Author(s) 2018. CC BY 4.0 License.

Pine Island and Thwaites glaciers, West Antarctica, with airborne observations of snow accumulation, The Cryosphere, 8, 1375–1392, https://doi.org/10.5194/tc-8-1375-2014, 2014.

Millan, R., Rignot, E., Bernier, V., Morlighem, M., and Dutrieux, P.: Bathymetry of the Amundsen Sea Embayment sector of West Antarctica from Operation IceBridge gravity and other data, Geophys. Res. Lett., 44, 1360–1368, https://doi.org/10.1002/2016GL072071, 2017.

Morland, L. W.: Unconfined ice shelf flow, Proceedings of Workshop on the Dynamics of the West Antarctic Ice Sheet, University of Utrecht, May 1985. Published by Reidel, ed. C.J. v, 99–116, 1987.

Morlighem, M., Rignot, E., Seroussi, H., Larour, E., Ben Dhia, H., and Aubry, D.: Spatial patterns of basal drag inferred using control methods from a full-Stokes and simpler models for Pine Island Glacier, West Antarctica, Geophys. Res. Lett., 37, L14 502, 2010.

Morlighem, M., Rignot, E., Seroussi, H., Larour, E., Ben Dhia, H., and Aubry, D.: A mass conservation approach for mapping glacier ice thickness, Geophys. Res. Lett., 38, 1–6, https://doi.org/10.1029/2011GL048659, 2011.

Morlighem, M., Seroussi, H., Larour, E., and Rignot, E.: Inversion of basal friction in Antarctica using exact and incomplete adjoints of a higher-order model, J. Geophys. Res., 118, 1746–1753, https://doi.org/10.1002/jgrf.20125, 2013.

Mouginot, J., Rignot, E., and Scheuchl, B.: Sustained increase in ice discharge from the Amundsen Sea Embayment, West Antarctica, from 1973 to 2013, Geophys. Res. Lett., 41, 1–9, https://doi.org/10.1002/2013GL059069, 2014.

Nowicki, S. M. J. and Wingham, D. J.: Conditions for a steady ice sheet–ice shelf junction, Earth Planet. Sci. Lett., 265, 246–255, https://doi.org/10.1016/j.epsl.2007.10.018, 2008.

Parizek, B. R., Christianson, K., Anandakrishnan, S., Alley, R. B., Walker, R. T., Edwards, R. a., Wolfe, D. S., Bertini, G. T., Rinehart, S. K., Bindschadler, R. a., and Nowicki, S. M. J.: Dynamic (in)stability of Thwaites Glacier, West Antarctica, J. Geophys. Res., 118, 1–18, https://doi.org/10.1002/jgrf.20044, 2013.

Pattyn, F.: A new three-dimensional higher-order thermomechanical ice sheet model: Basic sensitivity, ice stream development, and ice flow across subglacial lakes, J. Geophys. Res., 108, 1–15, https://doi.org/10.1029/2002JB002329, 2003.

Pattyn, F., Perichon, L., Durand, G., Favier, L., Gagliardini, O., Hindmarsh, R. C. A., Zwinger, T., Albrecht, T., Cornford, S., Docquier, D., Fuerst, J., Goldberg, D., Gudmundsson, H., Humbert, A., Hutten, M., Huybrecht, P., Jouvet, G., Kleiner, T., Larour, E., Martin, D., Morlighem, M., Payne, A. J., Pollard, D., Ruckamp, M., Rybak, O., Seroussi, H., Thoma, M., Wilkens, N., Fu, J. J., Gudmundsson, G. H., Huybrechts, P., and Ru, M.: Grounding-line migration in plan-view marine ice-sheet models: results of the ice2sea MISMIP3d intercomparison, J. Glaciol., 59 (215), 410–422, https://doi.org/10.3189/2013JoG12J129, 2013.

Pollard, D., Deconto, R. M., and Alley, R. B.: Potential Antarctic Ice Sheet retreat driven by hydrofracturing and ice cliff failure, Earth Planet. Sci. Lett., 412, 112–121, https://doi.org/10.1016/j.epsl.2014.12.035, http://dx.doi.org/10.1016/j.epsl.2014.12.035, 2015.

Pritchard, H. D., Arthern, R. J., Vaughan, D. G., and Edwards, L. A.: Extensive dynamic thinning on the margins of the Greenland and Antarctic ice sheets, Nature, 461, 971–975, https://doi.org/10.1038/nature08471, 2009.

Rignot, E.: Evidence for rapid retreat and mass loss of Thwaites Glacier, West Antarctica, J. Glaciol., 47, 213–222, https://doi.org/10.3189/172756501781832340, 2001.

Rignot, E.: Changes in West Antarctic ice stream dynamics observed with ALOS PALSAR data, Geophys. Res. Lett., 35, 1–5, https://doi.org/10.1029/2008GL033365, 2008.

Rignot, E., Mouginot, J., and Scheuchl, B.: Antarctic grounding line mapping from differential satellite radar interferometry, Geophys. Res. Lett., 38, https://doi.org/10.1029/2011GL047109, 2011a.

Rignot, E., Mouginot, J., and Scheuchl, B.: Ice Flow of the Antarctic Ice Sheet, Science, 333, 1427–1430, https://doi.org/10.1126/science.1208336, 2011b.

© Author(s) 2018. CC BY 4.0 License.

Rignot, E., Jacobs, S., Mouginot, J., and Scheuchl, B.: Ice shelf melting around Antarctica, Science, 341, 266–270, https://doi.org/10.1126/science.1235798, 2013.

Rignot, E., Mouginot, J., Morlighem, M., Seroussi, H., and Scheuchl, B.: Widespread, rapid grounding line retreat of Pine Island, Thwaites, Smith, and Kohler glaciers, West Antarctica, from 1992 to 2011, Geophys. Res. Lett., 41, 3502–3509, https://doi.org/10.1002/2014GL060140, 2014.

Scambos, T. A., Bell, R. E., Alley, R. B., Anandakrishnan, S., Bromwich, D. H., Brunt, K., Christianson, K., Creyts, T., Das, S. B., DeConto, R., Dutrieux, P., Fricker, H. A., Holland, D., MacGregor, J., Medley, B., Nicolas, J. P., Pollard, D., Siegfried, M. R., Smith, A. M., Steig, E. J., Trusel, L. D., Vaughan, D. G., and Yager, P. L.: How much, how fast?: A science review and outlook for research on the instability of Antarctica's Thwaites Glacier in the 21st century, Global and Planetary Change, 153, 16–34, https://doi.org/10.1016/j.gloplacha.2017.04.008, 2017.

Schneider, D. P. and Steig, E. J.: Ice cores record significant 1940s Antarctic warmth related to tropical climate variability., Proc. Natl. Acad. Sci. USA, 105, 12 154–12 158, https://doi.org/10.1073/pnas.0803627105, 2008.

Schodlok, M. P., Menemenlis, D., Rignot, E., and Studinger, M.: Sensitivity of the ice-shelf/ocean system to the sub-ice-shelf cavity shape measured by NASA IceBridge in Pine Island Glacier, West Antarctica, Ann. Glaciol., 53(60), 156–162, https://doi.org/10.3189/2012AoG60A073, 2012.

Schoof, C.: Ice sheet grounding line dynamics: Steady states, stability, and hysteresis, J. Geophys. Res., 112, 1–19, https://doi.org/10.1029/2006JF000664, 2007.

Seroussi, H., Morlighem, M., Rignot, E., Larour, E., Aubry, D., Ben Dhia, H., and Kristensen, S. S.: Ice flux divergence anomalies on 79north Glacier, Greenland, Geophys. Res. Lett., 38, 1–5, 2011.

Seroussi, H., Ben Dhia, H., Morlighem, M., Rignot, E., Larour, E., and Aubry, D.: Coupling ice flow models of varying order of complexity with the Tiling Method, J. Glaciol., 58 (210), 776–786, https://doi.org/10.3189/2012JoG11J195, 2012.

Seroussi, H., Morlighem, M., Rignot, E., Khazendar, A., Larour, E., and Mouginot, J.: Dependence of century-scale projections of the Greenland ice sheet on its thermal regime, J. Glaciol., 59, 1024–1034, https://doi.org/10.3189/2013JoG13J054, 2013.

Seroussi, H., Morlighem, M., Larour, E., Rignot, E., and Khazendar, A.: Hydrostatic grounding line parameterization in ice sheet models, The Cryosphere, 8, 2075–2087, 2014.

Seroussi, H., Nakayama, Y., Larour, E., Menemenlis, D., Morlighem, M., Rignot, E., and Khazendar, A.: Continued retreat of Thwaites Glacier, West Antarctica, controlled by bed topography and ocean circulation, Geophys. Res. Lett., https://doi.org/10.1002/2017GL072910, 2017.

Shapiro, N. M. and Ritzwoller, M. H.: Inferring surface heat flux distributions guided by a global seismic model: particular application to Antarctica, Earth Planet. Sci. Lett., 223, 213–224, https://doi.org/10.1016/j.epsl.2004.04.011, 2004.

Spence, P., Griffie, S. M., England, M. H., Hogg, A. M., Saenko, O. A., and Jourdain, N. C.: Rapid subsurface warming and circulation changes of Antarctic coastal waters by poleward shifting winds, Geophys. Res. Lett., 41, 4601–4610, https://doi.org/10.1002/2014GL060613.Received, 2014.

Tsai, V. C., Stewart, A. L., and Thompson, A. F.: Marine ice-sheet profiles and stability under Coulomb basal conditions, J. Glaciol., 61, 205–215, https://doi.org/10.3189/2015JoG14J221, 2015.

van der Veen, C. J. and Whillans, I. M.: Force budget: I. Theory and numerical methods, J. Glaciol., 35, 53–60, 1989.

Vieli, A. and Payne, A. J.: Assessing the ability of numerical ice sheet models to simulate grounding line migration, J. Geophys. Res., 110, F01 003, https://doi.org/10.1029/2004JF000202, 2005.

© Author(s) 2018. CC BY 4.0 License.

Weertman, J.: On the sliding of glaciers, J. Glaciol., 3, 33–38, 1957.

Weertman, J.: Stability of the junction of an ice sheet and an ice shelf, J. Glaciol., 13(67), 3–11, 1974.

Wise, M. G., Dowdeswell, J. A., Jakobsson, M., and Larter, R. D.: Evidence of marine ice-cliff instability in Pine Island Bay from iceberg-keel plough marks, Nature, 550, 506–510, https://doi.org/10.1038/nature24458, 2017.

Yu, H., Rignot, E., Morlighem, M., and Seroussi, H.: Iceberg calving of Thwaites Glacier, West Antarctica: Full-Stokes modeling combined with linear elastic fracture mechanics, The Cryosphere, 11, 1283–1296, https://doi.org/10.5194/tc-11-1283-2017, 2017.